

Amperometric Determination of Hydroquinone and Catechol Based on Nanodiamond Powder Electrode

Linyan Bian¹, Haitao Zong^{2,*}, Chunli Li¹, Jianbing Zang³, Yanhui Wang³, Dafeng Zhang¹, Yang Li¹

¹ School of Chemistry and Chemical Engineering, Henan Polytechnic University, Jiaozuo, Henan, 454000, China

² School of Physics and Electronics Information, Henan Polytechnic University, Jiaozuo, Henan, 454000, China

³ State Key Lab of Metastable Materials Science and Technology, and College of Materials Science and Engineering, Yanshan University, Qinhuangdao, Hebei, 066004, China

*E-mail: haitaozong@163.com

Received: 8 June 2018 / Accepted: 12 August 2018 / Published: 30 November 2018

In this work, nanodiamond (ND) powder electrodes were fabricated and the electrochemical properties were investigated in the solution containing hydroquinone and catechol in 0.1M phosphate buffer solution (pH 7.0). Both hydroquinone and catechol exhibited well-defined redox peaks and much larger peak currents at ND powder electrodes. Under the optimized condition, the amperometric current response on ND powder electrodes were linear over ranges from 2.0×10^{-6} M to 1.0×10^{-4} M for hydroquinone, and from 4.0×10^{-6} M to 9.0×10^{-5} M for catechol, with the detection limits of 8.1×10^{-7} M and 4.2×10^{-7} M, respectively. Our current work suggested that ND powder electrodes had much potential to be applied in the detection of phenolic organic compounds.

Keywords: nanodiamond, hydroquinone, catechol, determination.

1. INTRODUCTION

Hydroquinone (1,4-dihydroxybenzene, HQ) and catechol (1,2-dihydroxybenzene, CC) are phenolic compounds and widely used in the production of dyes, cosmetics, pesticides and pharmaceuticals. Also, HQ and CC are two important environmental pollutants due to their high toxicity and low degradability[1] in the ecological circumstance[2]. Furthermore, these two dihydroxybenzene isomers usually coexist and interfere with each other during their determination because of their similar structures and properties. The acceptable emission of phenolic compounds according to the national standard of China (GB 8978-1996) is 0.5 mg/L (for dihydroxybenzene, 0.00454 M)[3]. Therefore, it is necessary to develop a simple, fast and reliable analytical method for simultaneous determination of HQ and CC[4,5]. Up to now, numerous methods have been exploited for their determination, including synchronous

fluorescence technique[6], spectrophotometry[7], gas chromatography[8], pH-based flow injection analysis[9] and liquid chromatography[10] and electrochemical methods[11-14].

Recently, electrochemical methods have attracted increasing attentions owing to the advantages of low cost, fast response, excellent selectivity, and high sensitivity. Carbon-based electrodes have been widely used in electrochemistry because of their chemical inertness, wide potential window and suitability for different types of analysis[15]. Over the past ten years, several carbon-based electrodes including carbon fiber electrode[16], carbon nanotubes (CNT)-modified electrode[17–22], and boron-doped diamond (BDD) electrode[23,24] have been investigated for dihydroxybenzene sensor. The early investigation concerning the simultaneous electrochemical determination of the two isomers was conducted at a glassy carbon electrode modified with multi-walled carbon nanotubes (MWCNTs) and yield promising results[17,18].

Unlike sp^2 -bonded carbon materials, diamond possesses a valence bond structure of sp^3 -bonded, and which makes it exhibit good physical stability and chemical stability under high potential, acidic and alkaline conditions. ND is a special form of diamond material and has the advantages of diamond. Besides, ND also exhibits excellent electrochemical properties in solution due to nano-size effect. In previous studies, ND was used for the determination of nitrite[25] and electrocatalytic oxidation of methanol as catalyst carrier[26-29]. In our present study, ND powder electrode was prepared and used for the determination of HQ and CC.

2. EXPERIMENTAL

2.1. Materials

ND powder with an average particle size of 100 nm was fabricated by mechanical crushing and was supplied by square and circle of Tuocheng Co.. Hydroquinone (HQ) and catechol (CC) were purchased from Tianjin, China. All reagents were of analytical grade and deionized water was used to prepare the solutions. The 0.1 M phosphate buffer solution (PBS) (pH 7.0) prepared using a combination of NaH_2PO_4 , Na_2HPO_4 , and NaCl was employed as a supporting electrolyte.

2.2. Experimental measurements

All the electrochemical experiments were performed using the CHI760D electrochemical workstation (Shanghai Chenhua Co., China) in a conventional three-electrode configuration. Platinum electrode, Ag/AgCl electrode (in saturated KCl solution), and ND powder electrode were applied as counter, reference, and working electrodes, respectively. The ND powder electrode was obtained as follows: (1) The bare glassy carbon electrode (GC) was polished successively using 0.3 and 0.05 mm alumina slurries. After 3 min of ultrasonication in ethanol and water successively, the electrode was rinsed with water for several times and then dried. (2) ND powder (about 10 mg) were dispersed in 10 mL deionized water by ultrasonication for 30 min to achieve a 1.0 mg/mL suspension. (3) one drop (5 μL) of the suspension was directly cast on the surface of the GC (2 mm in diameter) and evaporated at room temperature.

3. RESULTS AND DISCUSSION

Fig. 1 showed the cyclic voltammograms of 0.1 M PBS at the GC and ND/GC electrodes. It can be seen that both GC electrode and ND/GC electrode exhibit similar electrochemical properties and the potential window ranged from -0.3 V to $+1.0$ V. Besides, there was no peak in the electric potential platform, which can provide a good platform for the detection of potential.

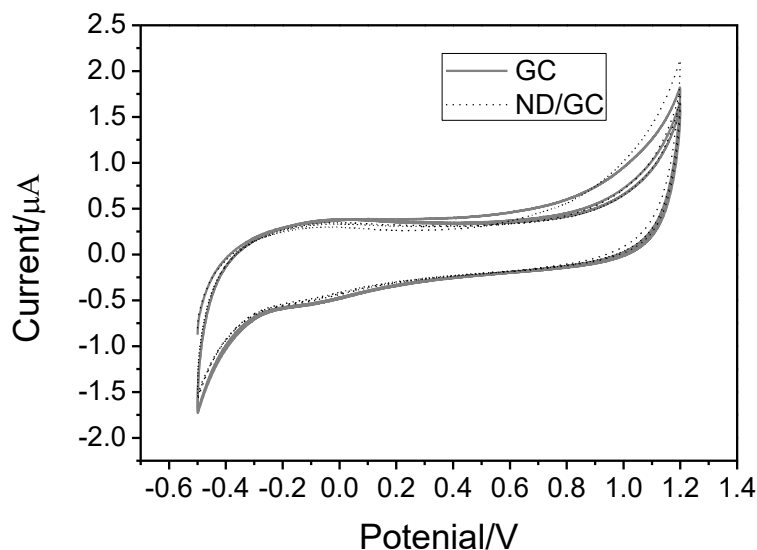


Figure 1. Cyclic voltammetry of GC and ND/GC in 0.1 M PBS (pH 7.0). Scan rate: 0.1 V/s.

Fig. 2 (A) displays the differential pulse voltammetry (DPV) curves of ND/GC in 0.1 M PBS (a) and 10 μ M CC (c) and DPV curve of GC in 10 μ M CC (b). At bare GC (curve b), the electrooxidation of the CC presents only a small peak ($I_p=0.056$ μ A) at 0.15V. Compared with bare GC, a well-defined oxidation peak with large peak current ($I_p=1.666$ μ A) for CC are observed at ND/GC (curve c) when potential was 0.15 V, indicating the excellent electrochemical response of ND/GC electrode even the concentration of CC was as low as 10 μ M. Therefore, it can be clearly inferred that the electrochemical response of ND/GC electrode to CC should be mainly attributed to ND.

Fig. 2 (B) was the DPV curves of ND/GC in 0.1 M PBS (a) and 10 μ M HQ (c) and DPV curve of GC in 10 μ M HQ (b). For the ND/GC electrode (curve c), it can be seen that there was an oxidation peak with a peak current I_p of 1.428 μ A can be observed in the 10 μ M HQ solution while the potential was 0.03 V. For the GC electrode (curve b), the peak current of the oxidation peak in the 10 μ M HQ solution was 0.126 μ A and one order of magnitude smaller than that of the ND/GC electrode. Hence, based on the comprehensive analysis of the DPV curves in Fig. 2 (A) and (B), we can draw a clear conclusion that ND has excellent electrochemical response to both CC and HQ. This improvement in electron transfer kinetics could be explained as follow: the nanometer size, large surface area, and surface functional groups of ND powder could enhance the performance of the peroxide oxidation process of CC and HQ on the ND/GC electrode and reduce the charge transfer resistance, thus improving its reversibility which greatly enhanced the peak currents[30].

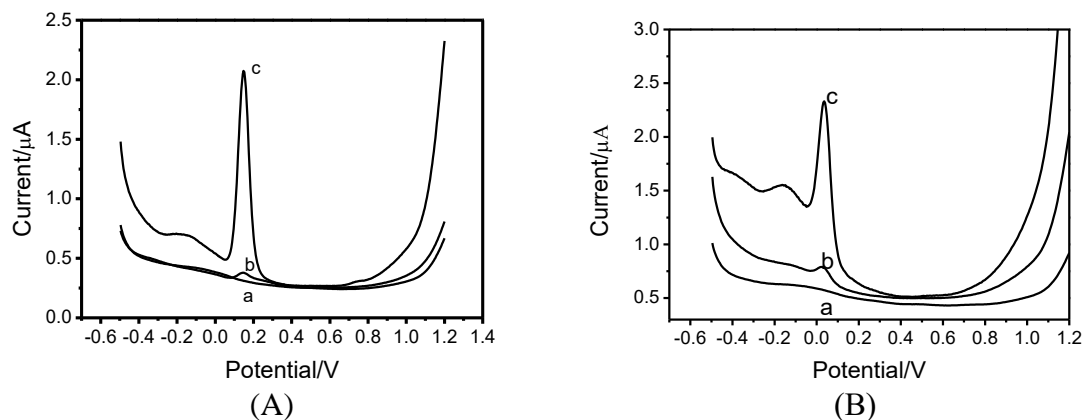


Figure 2. (A) DPVs of ND/GC in 0.1 M PBS (curve a) and 10 μM CC (curve c) and DPV of GC in 10 μM CC (curve b), (B) DPVs of ND/GC in 0.1 M PBS (curve a) and 10 μM HQ (curve c) and DPV of GC in 10 μM HQ (curve b)

The electrocatalytic oxidation of CC and HQ at the ND/GC electrode was also investigated by DPV in PBS (pH 7.0) at a scan rate of 50 mV/s by varying their concentrations (Fig. 3A and 3B). With an increase in the concentration of analytes, oxidation peak currents of CC and HQ increase. To verify the linear relationship between oxidation peak currents and CC and HQ concentrations, calibration curves were constructed. The peak currents increase linearly with increase in the concentration of CC and HQ. A linear dynamic range and a calibration equation were obtained for CC (Fig. 3A), $4.0 \times 10^{-6} \sim 9.0 \times 10^{-5}$ M, $I_{pc} (\mu\text{A}) = 0.1822C (\mu\text{M}) - 0.0782$ ($R^2 = 0.99617$); for HQ (Fig. 3B), $2.0 \times 10^{-6} \sim 1.0 \times 10^{-4}$ M, $I_{pc} (\mu\text{A}) = 0.2410C (\mu\text{M}) - 0.19536$ ($R^2 = 0.97884$). The detection limit of 4.29×10^{-7} M and 8.1×10^{-7} M ($S/N = 3$) was obtained for CC and HQ respectively.

A comparison of the proposed electrode with other carbon-based modified electrode is listed in Table 1. As can be observed, the detection limit for both HQ and CC are lower than those obtained at the MWCNT-PMG/GC [31] and PASA/MWNT/GC [2], and their linear ranges are wider than those obtained at BG[32] and SWNT/GC [19], indicating that the proposed sensor have rational linear ranges and acceptable detection limits. Although the sensing properties of detection limit and sensitivity of ND powder are not the best compared with some previous works, while the sensing performance of the obtained ND could be further improved by surface modification, such as coating noble metal nanoparticles and surface carbonation. Therefore, the improved electrode can be applied as a promising electrode for simultaneous and sensitive determination of HQ and CC without interference with each other.

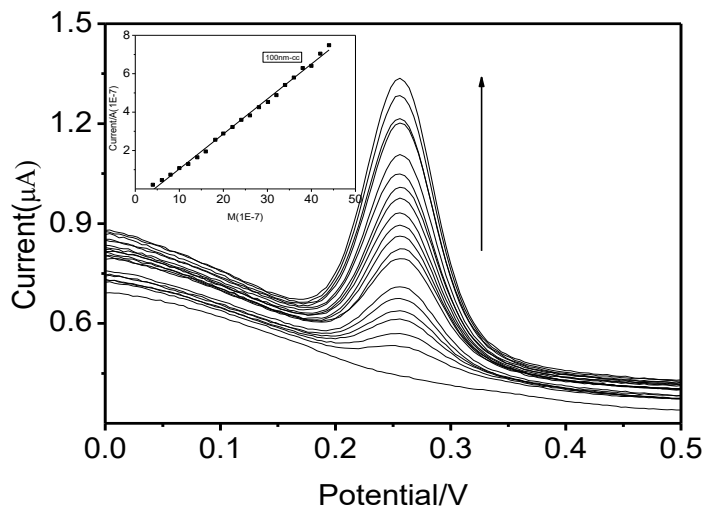


Figure 3A. DPVs at ND/GC electrode in CC by varying the concentration from 0.4 to 4.4 μM . The curves from the bottom to the top correspond to the concentration of 2, 4, 6, 8, 10, 12, 14, 16, 18, 20, 22, 24, 26, 28, 30, 32, 34, 36, 38 and 40 μM , respectively. Inset shows the calibration plot of CC.

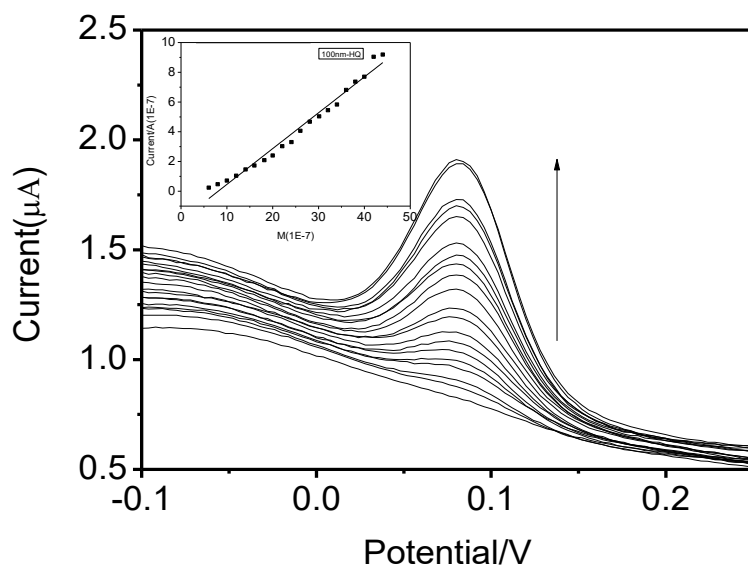


Figure 3B. DPVs at ND/GC electrode in HQ by varying the concentration from 0.4 to 4.4 μM . The curves from the bottom to the top correspond to the concentration of 2, 4, 6, 8, 10, 12, 14, 16, 18, 20, 22, 24, 26, 28, 30, 32, 34, 36, 38 and 40 μM , respectively. Inset shows the calibration plot of HQ

Table 1. Comparison of major characteristics of various dihydroxybenzene isomers sensors.

Electrode material	Isomer	Linear range (μM)	Detection limit (μM)	Reference
ECF-CPE ^a	HQ	1-200	0.4	[14]
	CC	1-200	0.2	
BG ^b	HQ	5-100	0.3	[32]

	CC	1-75	0.2	
LRG ^c	HQ	1-300	0.5	[33]
	CC	3-300	0.8	
MWNT ^d	HQ	1-100	0.75	[18]
	CC	6-100	0.2	
MWCNT-PMG ^e /GC	HQ	10-480	1.6	[31]
	CC	30-1190	5.8	
PASA ^f /MWNT/GC	HQ	6-400	1.0	[2]
	CC	6-700	1.0	
SWNT ^g /GC	HQ	0.4-10	0.12	[19]
	CC	0.4-10	0.26	
ND	HQ	2-100	0.81	This work
	CC	4-90	0.42	

^a ECF-CPE: electrospun carbon nanofiber-modified carbon paste electrode.

^b BG: Boron-doped graphene.

^c LRG: Laser reduced graphene.

^d MWNT: Multiwall carbon nanotubes.

^e MWCNT-PMG: Multiwall carbon nanotubes-polymalachite.

^f PASA: Poly-amidosulfonic acid.

^g SWNT: Single-walled carbon nanotube.

The pH value of the PBS has significant impact on the detection of CC and HQ. Therefore, the effect of solution pH on the response of CC and HQ was investigated in the range of 5.0–9.0. The DPVs of 0.1 M CC and 0.1 M HQ at ND/GC electrodes in 0.1 M PBS with different pH (5.0, 6.0, 7.0, 8.0 and 9.0) were shown in Fig. 4A and Fig. 4B, respectively. The peak currents of CC and HQ in PBS solutions with different pH were shown in Fig. 4C. It can be seen that for both CC and HQ, the peak current increased first and then decreased with the increase of pH value and the maximum response were found at pH 7.0. The reason for the phenomenon could be attributed to the large amount of functional groups containing oxygen and nitrogen absorbed on the surface of ND powder. With the pH increased from 5.0 to 7.0, the dissociation degrees of the oxygen-containing groups increased and the hydrogen bonding of hydroxyl in oxygen-containing groups and dihydroxybenzene enhanced, which can increase the adsorption capacity of dihydroxybenzene isomers on the surface of ND/GC electrode and thus the response current increased. When the pH was larger than 7.0, due to the attraction between OH⁻ and phenolic hydroxyl groups in the solution, the formation of hydrogen bond on the surface of ND/GC electrode and phenolic hydroxyl group was weakened and therefore the oxidation peak current was reduced or even disappeared. Additionally, the relationship between the oxidation peak potential and pH was also investigated (Fig. 4D). It was found that the oxidation peak potentials shift negatively while pH increased from 5.0 to 9.0 for both CC and HQ, indicating that high pH was beneficial to the electrochemical reaction. The linear regression equations for oxidation peak potentials and pH were E(V)

= $0.5112 - 0.049 \text{ pH}$, ($R^2=0.98687$) and $E(V) = 0.042 - 0.053 \text{ pH}$, ($R^2=0.99179$) for CC and HQ, respectively. The slopes of the two regression equations for CC and HQ were -49 mV/pH and -53 mV/pH , respectively. It should be noted that the slopes of the equations were very close to the theory value of -59 mV/pH [34], suggesting that the electrochemical redox process of CC and HQ at ND was a two-electron and two-proton process[18] (as shown in Scheme 1). Therefore, in order to achieve high sensitivity, pH 7.0 was chosen for the simultaneous determination of CC and HQ.

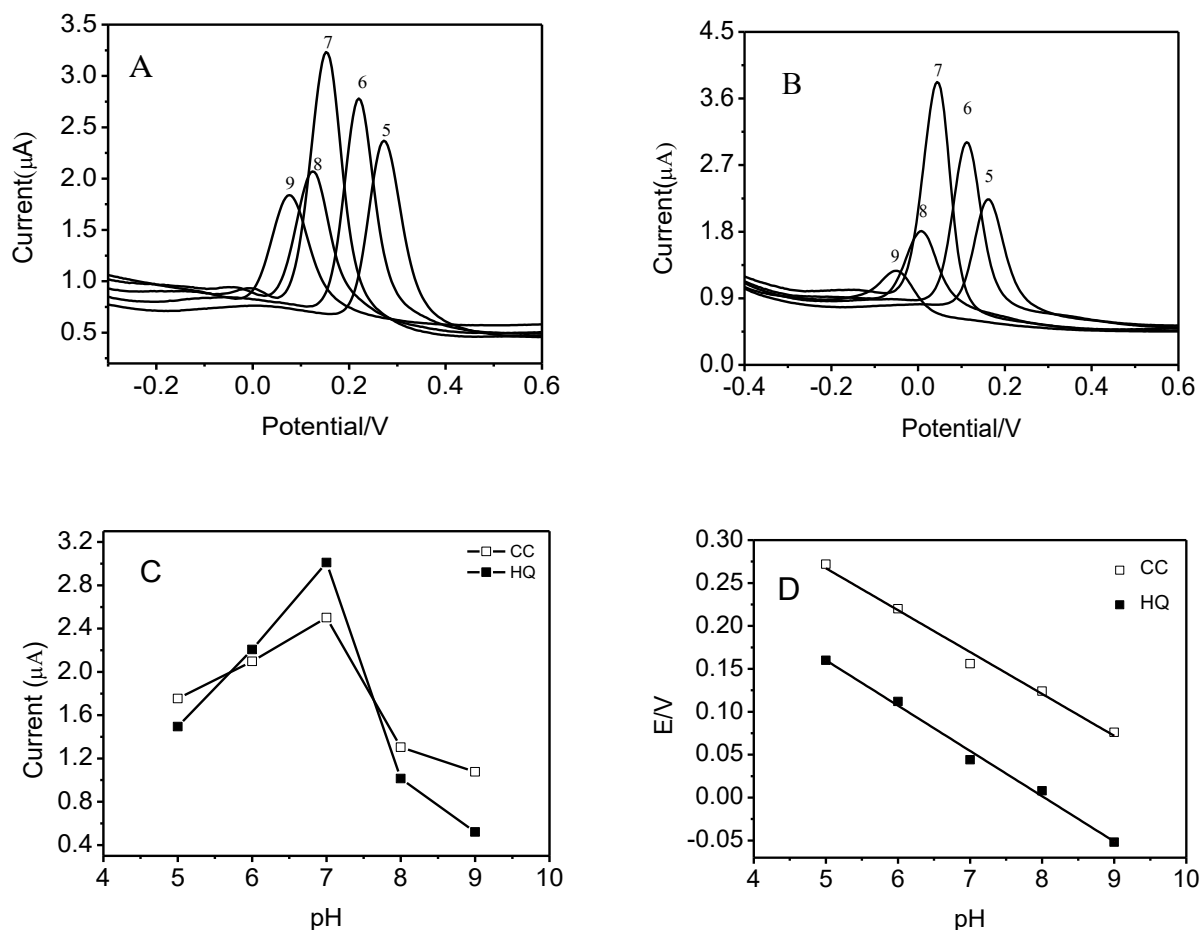
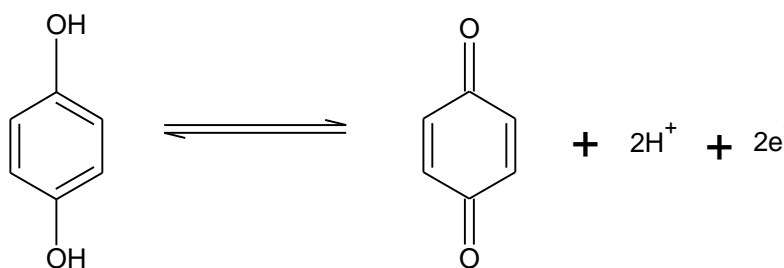
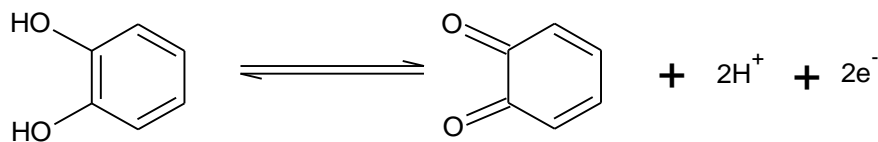


Figure 4. DPVs of (A) 0.1mM CC and (B) 0.1mM HQ at ND/GC in 0.1M PBS with different pH:5.0, 6.0, 7.0, 8.0, 9.0; effect of pH value on (C) the anodic peak currents and (D) anodic peak potential of HQ and CC.





Scheme 1. The expected mechanism of HQ and CC at ND/GC

The DPV curves of ND/GC electrode (a) and GC electrode (b) in 0.1 M PBS (pH 7.0) containing 0.1mM CC and 0.1mM HQ were shown in Fig. 5. As shown in Fig. 5 (curve b), there is a broad oxidation peak at potentials around +0.15 V for bare GC electrode, which indicates the oxidation peaks of CC and HQ overlapped to form a wide peak, therefore, it was impossible to simultaneously determine CC and HQ using bare GC. In contrast, two well-defined oxidation peaks with much larger current response at potentials of +0.088 V and +0.198V for HQ and CC are observed at ND/GC (curve a). The probable reason for the peak separation is that the electron cloud density is lower from HQ to CC, so the oxidation of HQ is easier than that of CC, which is similar with the previous report [11,17]. In addition, the ND/GC electrode facilitates electron transfer and increased electrochemistry signals of CC and HQ, which could be attributed to the large surface area and surface functional groups of ND powder. Thus, the ND/GC shows excellent selectivity and sensitivity in the simultaneous determination of CC and HQ.

Fig. 6 showed the DPV curves of ND/GC electrode in the mixed solution of CC and HQ with different concentrations. The concentrations of CC and HQ from bottom to top were 0.5 mM, 0.01mM, 0.05 mM and 0.1 mM, respectively. Two well-defined oxidation peaks with large peak separation at the potential of 0.088 V (for CC) and 0.198 V (for HQ) can be found under all concentrations, further confirmed that ND/GC electrode has excellent detecting sensitivity to CC and HQ mixed solution.

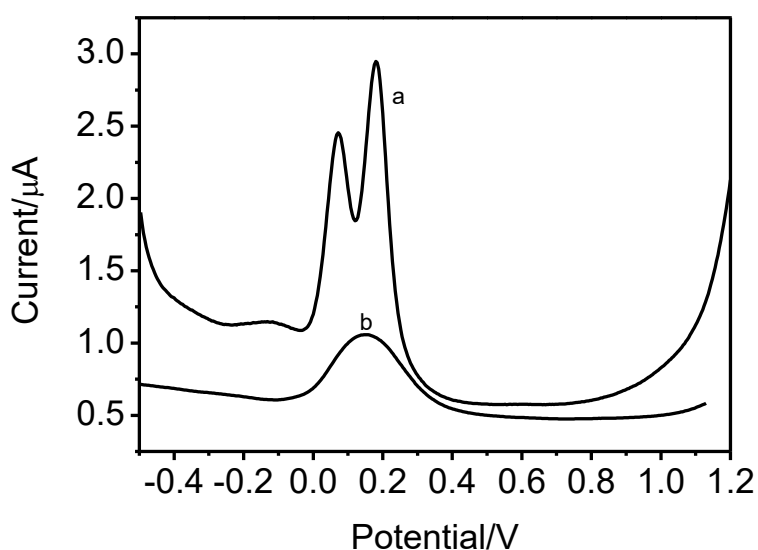


Figure 5. DPV of ND/GC(a) and GC (b) in 0.1 M PBS (pH 7.0) containing 0.1mM CC and 0.1mM HQ

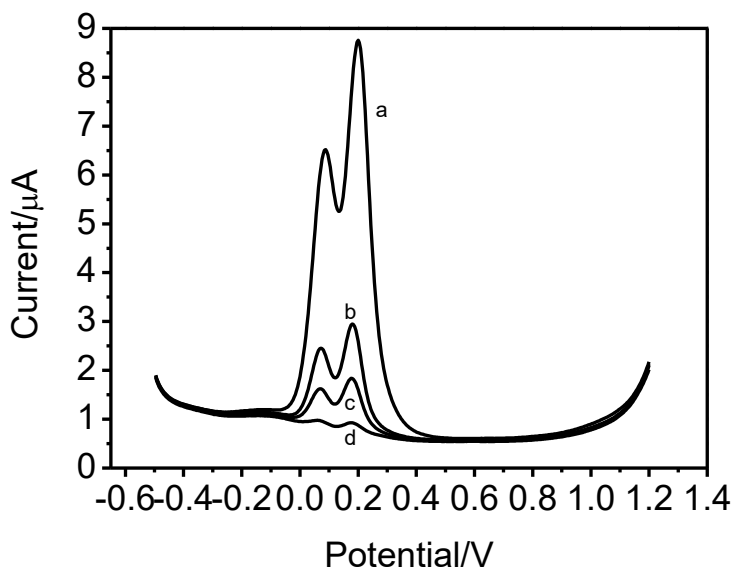


Figure 6. DPV of ND/GC in 0.1 M PBS (pH 7.0) containing (a) 0.5mM CC and 0.5mM HQ and (b) 0.1mM CC and 0.1 mM HQ and (c) 0.05 mM CC and 0.05 mM HQ and (d) 0.01 mM CC and 0.01 mM HQ.

4. CONCLUSION

In this paper, ND powder electrode with low cost had been fabricated by a simple and feasible method. The ND powder electrode exhibited an excellent electrocatalytic activity toward the oxidation of HQ and CC. A wider concentration linear range, lower detection limit and good detection selectivity for HQ and CC mixed solution were achieved on the ND powder electrode. Also, coupled with the unique chemical and physical stability of diamond, ND powder electrodes are expected to be applied in the detection of phenolic organic compounds.

ACKNOWLEDGMENT

This work was supported by National Natural Science Foundation of China (No.51302066).

References

1. A.L. Buikema Jr., M.J. Mc Ginniss, *Mar. Environ. Res.*, 2 (1979) 87.
2. D.M. Zhao, X.H. Zhang, L.J. Feng, S.F. Wang, *Colloids Surf., B*, 74 (2009) 317.
3. H. Yin, Q. Zhang, Y. Zhou, Q. Ma, T. liu, L. Zhu, S. Ai, *Electrochim. Acta*, 56 (2011) 2748.
4. A. Ahammad, S. Sarker, M.A. Rahman, J.J. Lee, *Electroanalysis*, 22 (2010) 694.
5. L.Z. Zheng, L.Y. Xiong, Y.D. Li, J.P. Xu, X.W. Kang, Z.J. Zou, S.M. Yang, J. Xia, *Sens. Actuators, B*, 177 (2013) 344.
6. M. Pistonesi, M. Di Nezio, M. Centurión, M. Palomeque, A. Lista, B. Fernández Band, *Talanta*, 69 (2006) 1265.
7. H. Cui, Q.L. Zhang, A. Myint, X.W. Ge, L.J. Liu, *J. Photochem. Photobiol., A*, 181 (2006) 238.
8. J.S. O'Grodnick, G.D. Dupre, B.J. Gulizia, S.H. Blake, *J. Chromatogr. Sci.*, 21 (1983) 289.

9. J.A. Garcia-Mesa, R. Mateos, *J. Agric. Food Chem.*, 55 (2007) 3863.
10. A. Asan, I. Isildak, *J. Chromatogr. A*, 988 (2003) 145.
11. K.Y. He, X.S. Wang, X.H. Meng, H.T. Zheng, Shin-ichiro, Suye, *Sens. Actuators, B*, 193 (2014) 212.
12. B. Unnikrishnan, Pu-Liang, Ru, Shen-Ming, Chen, *Sens. Actuators, B*, 169 (2012) 235.
13. Y.L. Zhang, S.X. Xiao, J.L. Xie, Z.M. Yang, P.F. Pang, Y.T. Gao, *Sens. Actuators, B*, 204 (2014) 102.
14. Q.H. Guo, J.S. Huang, P.Q. Chen, Y. Liu, H.Q. Hou, T.Y. You, *Sens. Actuators, B*, 163 (2012) 179.
15. X.F. Tang, Y. Liu, H.Q. Hou, T.Y. You, *Talanta*, 80 (2010) 2182.
16. R.M. de Carvalho, C. Mello, L.T. Kubota, *Anal. Chim. Acta*, 420 (2000) 109.
17. Y.P. Ding, W.L. Liu, Q.S. Wu, X.G. Wang, *J. Electroanal. Chem.*, 575 (2005) 275.
18. H.L. Qi, C.X. Zhang, *Electroanalysis*, 17 (2005) 832.
19. Z.H. Wang, S.J. Li, Q.Z. Lv, *Sens. Actuators, B*, 127 (2007) 420.
20. S.G. Wang, Y.Q. Li, X.J. Zhao, J.H. Wang, J.J. Han, T. Wang, *Diamond Relat. Mater.*, 16 (2007) 248.
21. D.D. Zhang, Y.G. Peng, H.L. Qi, Q. Gao, C.X. Zhang, *Sens. Actuators, B*, 136 (2009) 113.
22. Z.A. Xu, X. Chen, X.H. Qu, S.J. Dong, *Electroanalysis*, 16 (2004) 684.
23. Y.Z. Lei, G.H. Zhao, M.C. Liu, X.E. Xiao, Y.T. Tang, D.M. Li, *Electroanalysis*, 19 (2007) 1933.
24. M. Lv, M. Wei, F. Rong, C. Terashima, A. Fujishima, Z.Z. Gu, *Electroanalysis*, 22 (2010) 199.
25. L.H. Chen, J.B. Zang, Y.H. Wang, L.Y. Bian, *Electrochim. Acta*, 53 (2008) 3442.
26. Y. Zhang, Y.H. Wang, L.Y. Bian, R. Lu, J.B. Zang, *Int. J. Hydrogen Energy*, 41 (2016) 4624.
27. L.Y. Bian, Y.H. Wang, J.B. Zang, F.W. Meng, Y.L. Zhao, *Int. J. Hydrogen Energy*, 37 (2012) 1220.
28. L.Y. Bian, Y.H. Wang, J.B. Zang, J.K. Yu, H. Huang, *J. Electroanal. Chem.*, 644 (2010) 85.
29. J.B. Zang, Y.H. Wang, L.Y. Bian, J.H. Zhang, F.W. Meng, Y.L. Zhao, R. Lu, X.H. Qu, S.B. Ren, *Carbon*, 50 (2012) 3032.
30. X. Wang, M. Wu, H. Li, Q. Wang, P. He, Y. Fang, *Sens. Actuators, B*, 192 (2014) 452.
31. Y. Umasankar, A.P. Periasamy, S.M. Chen, *Anal. Biochem.*, 411 (2011) 71.
32. Y.Z. Zhang, R.X. Sun, B.M. Luo, L.J. Wang, *Electrochim. Acta*, 156 (2015) 228.
33. T. Lai, W.H. Cai, W.L. Dai, J.S. Ye, *Electrochim. Acta*, 138 (2014) 48.
34. S.H. DuVall, R.L. McCreery, *Anal. Chem.*, 71 (1999) 4594.